© 2018. Published by The Company of Biologists Ltd | Journal of Experimental Biology (2018) 221, jeb189233. doi:10.1242/jeb.189233

RESEARCH ARTICLE

How do baleen whales stow their filter? A comparative biomechanical analysis of baleen bending

Alexander J. Werth[1,‡], Diego Rita[2], Michael V. Rosario[3,*], Michael J. Moore[4] and Todd L. Sformo[5,6]

ABSTRACT

Bowhead and right whale (balaenid) baleen filtering plates, longer in vertical dimension (≥3–4 m) than the closed mouth, presumably bend during gape closure. This has not been observed in live whales, even with scrutiny of video-recorded feeding sequences. To determine what happens to the baleen during gape closure, we conducted an integrative, multifactorial study including materials testing, functional (flow tank and kinematic) testing and histological examination. We measured baleen bending properties along the dorsoventral length of plates and anteroposterior location within a rack of plates via mechanical (axial bending, composite flexure, compression and tension) tests of hydrated and air-dried tissue samples from balaenid and other whale baleen. Balaenid baleen is remarkably strong yet pliable, with ductile fringes, and low stiffness and high elasticity when wet; it likely bends in the closed mouth when not used for filtration. Calculation of flexural modulus from stress/strain experiments shows that the balaenid baleen is slightly more flexible where it emerges from the gums and at its ventral terminus, but kinematic analysis indicates plates bend evenly along their whole length. Fin and humpback whale baleen has similar material properties but less flexibility, with no dorsoventral variation. The internal horn tubes have greater external and hollow luminal diameter but lower density in the lateral relative to medial baleen of bowhead and fin whales, suggesting a greater capacity for lateral bending. Baleen bending has major consequences not only for feeding morphology and energetics but also for conservation given that entanglement in fishing gear is a leading cause of whale mortality.

KEY WORDS: Cetacea, Mysticete, Jaw, Keratin, Filter feeding, Morphology, Flexibility, Stiffness

INTRODUCTION

Filtration is the most efficient means of collecting items suspended in water (Jorgensen, 1966; Rubenstein and Koehl, 1977). Many invertebrates use perforated bodies (e.g. tunicates) or antenna-like lophophores to capture food and transport it to the mouth, but adult vertebrates use internal filters (Lauder, 1985) within the buccal cavity, including the spined tongue of flamingos (Zweers et al., 1995), palatal lamellae of petrels (Prince and Morgan, 1987) and cusped teeth of crabeater seals (Bengtson and Stewart, 2018); or within the pharynx, as in gill rakers of large sharks and rays (Paig-Tran et al., 2013). A key question is whether the oral filter is rigid or flexible. Increased gape or other buccal/pharyngeal expansion exposes filtering surfaces to fluctuating prey flow, but does not generally require these filters to be compressed or flexed when not in use. Intraoral filtering surfaces usually remain fully extended during gape closure.

The flow of water through the oral filter of baleen whales (Mysticeti) may alter its porosity (Werth, 2013), but the oral filter is generally not compacted or otherwise changed in size, attitude or position when the mouth closes and the filter is not used. This is true in the largest mysticete species (rorquals of Family Balaenopteridae, including blue and humpback whales), the baleen plates of which average 30–60 cm in length (Young, 2012) and can be easily accommodated in a closed mouth with no physical alteration. However, plates are much longer, often ≥3–4 m (Werth, 2000, 2001), in bowhead (*Balaena mysticetus*) and right whales (*Eubalaena* spp.) of the Family Balaenidae. Balaenids feed by continuous, steady-state, ram-driven filtration, with their jaws abducted to partial or full (4–7 m) gape for extended periods during foraging (Werth, 2004; Werth and Potvin, 2016; Potvin and Werth, 2017). Although balaenid rostra exhibit marked dorsal arching (Fig. 1), this cranial modification is apparently insufficient to prevent the baleen from bending during jaw closure, as the full vertical span of the plates substantially exceeds the height of the closed mouth (2–3 m; Lambertsen et al., 1989; Fig. 1). This dilemma has long been recognized (Gray, 1877) but never investigated. Although balaenid plates presumably bend during gape closure, this has not been observed in live whales, even with close scrutiny of video-recorded feeding sequences.

The central issue here concerns material flexibility: inflexible items present hard limits when packed into a compartment such as the mouth, for they cannot exceed the compartment's dimensions, whereas softer items bend to pack a maximal volume into a minimal space. Baleen flexibility has not been the subject of systematic study, although it is generally recognized. Previous experiments (Werth et al., 2016a) showed the baleen is highly hydrophilic, absorbing one-third its mass in water. When rehydrated under realistic laboratory conditions (similar to those experienced *in vivo*), balaenid baleen is >10 times more flexible than the air-dried baleen familiar to most people, including scientists, from museum displays and collections (Werth et al., 2016a). Dried baleen is brittle whereas wet baleen is pliant. This change in the properties of baleen may not be surprising given the familiar softening effects of water on fingernails, another hard mammalian tissue composed solely of alpha-keratin (Forslind, 1970). Native artists who fashion baleen into baskets or decorations begin by rehydrating baleen to make it pliable (Lee, 1998). Once among the world's most valuable

[1]Department of Biology, Hampden-Sydney College, Hampden-Sydney, VA 23943, USA. [2]Department of Evolutionary Biology, Ecology, and Environmental Science, University of Barcelona, 08028 Barcelona, Spain. [3]Department of Ecology & Evolutionary Biology, Brown University, Providence, RI 02912, USA. [4]Biology Department, Woods Hole Oceanographic Institution, Woods Hole, MA 02543, USA. [5]Department of Wildlife Management, North Slope Borough, Barrow, AK 99723, USA. [6]Institute of Arctic Biology, University of Alaska Fairbanks, Fairbanks, AK 99775, USA.
*Present address: Department of Biology, West Chester University, West Chester, PA 19383, USA.

‡Author for correspondence (awerth@hsc.edu)

A.J.W., 0000-0002-7777-478X

Received 23 July 2018; Accepted 11 October 2018

Journal of Experimental Biology (2018) 221, jeb189233. doi:10.1242/jeb.189233

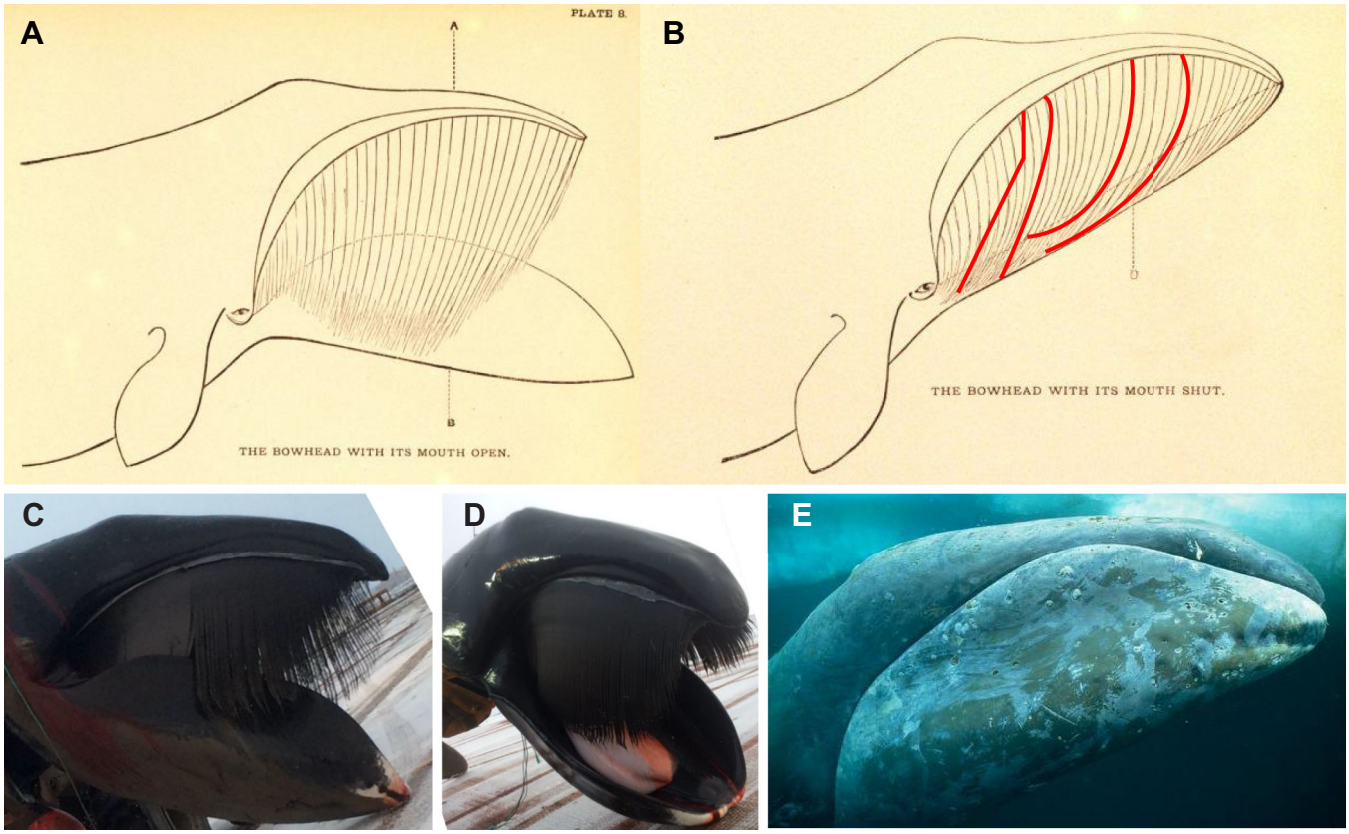

Fig. 1. Morphology of baleen bending. (A,B) Baleen plates of bowhead whales are longer than the height of the closed mouth and presumably bend to accommodate gape closure, as shown in these illustrations from Gray (1877). Red lines represent possible bending locations, including bending evenly along a plate's length or hinging at the top. It is uncertain whether all plates within a rack bend similarly. (C,D) Lateral (C) and anterolateral (D) views of fully opened mouths in hauled out bowheads indicate different plates might bend anteroposteriorly as well as mediolaterally to varying extents (photo credit: T.L.S.). (E) An underwater photo of a closed bowhead mouth (photo credit: ARKive.com, Martha Holmes) confirms the limited height of the balaenid mouth *in vivo*.

commodities (Stevenson, 1907), the durable strength and supple flexibility of 'whalebone' made it commercially useful for such products as corset stays, umbrellas, brushes, whips and even armor (Moffat et al., 2008).

Baleen is a neomorphic oral tissue with no functional analog or evolutionary homolog. Made entirely of epidermal alpha-keratin (Fraser et al., 1972, 1976; Marshall et al., 1991), it is anisotropic, with flat, nail-like cortical layers sandwiching a core of hollow, hair-like horn tubes plus intertubular medullary keratin fibers (Fig. 2). A whale's comb-like filtering apparatus comprises paired racks of

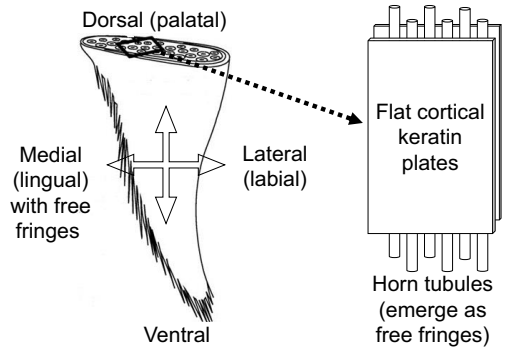

Fig. 2. Anatomical orientation of a representative baleen plate, with schematic model showing paired cortical plates enclosing tubular (and intertubular) keratin.

200–320 transversely oriented triangular plates that hang, suspended from palatal gingiva, like vertical blinds spaced ∼1 cm apart (Fig. 1). Baleen grows throughout life from gingival keratinocytes (Pinto and Shadwick, 2013); exposed baleen comprises dead, cornified cells and fibers. As baleen erodes from contact with prey, seawater and possibly abrasion from the tongue and other oral tissues (Werth et al., 2016b), horn tubes emerge, forming a mat-like mesh of intertwined fringes along a rack's medial (lingual) surface (Williamson, 1973; Pivorunas, 1976). Both plates and fringes comprise the filter (Werth, 2012; Jensen et al., 2017; Werth et al., 2018). Baleen grows throughout life at a rate of roughly 25–30 cm year^{-1} in right whales (Best and Schell, 1996; Hunt et al., 2016) and 15–20 cm year^{-1} in bowheads (Lubetkin et al., 2008) compared with 12–20 cm year^{-1} in rorquals (Eisenmann et al., 2016) and gray whales, *Eschrichtius* (Caraveo-Patiño et al., 2007). Thus, a 3-m-long right whale baleen plate exhibits 11 years of growth and a 4-m-long bowhead plate indicates 23 years. In contrast, rorqual/gray whale plates are estimated to reflect 3–5 years of growth (Rice and Wolman, 1971; Sumich, 2001; Aguilar et al., 2014).

The mechanical properties of mammalian keratinous tissues, especially wool fibers, whiskers, horns and hooves, have been widely studied (Feughelman, 1997, 2002; Hearle, 2000; Ginter-Summarell et al., 2015; Wang et al., 2016). Alpha-keratins are generally thought to be lighter and more flexible than steel, yet stronger and sturdier than other common biological materials including collagen-based connective tissues (Pautard, 1963; Bertram and Gosline, 1986, 1987;

McKittrick et al., 2012). Additionally, keratin provides waterproofing (similar to chitin) and is useful where water is frequently encountered (Kitchener and Vincent, 1987; Taylor et al., 2004; Greenberg and Fudge, 2012). Despite operating within the remarkably powerful forces and flows sustained by the highly dynamic environment – potentially filtering >100,000 l in 15–30 s in a large rorqual, with peak pressures reaching 800–1000 kPa or the equivalent of 8–10($\times10^5$) N m^{-2} (Werth, 2013) – the baleen nonetheless cannot clog or break and must remain functional for a century or more. Warped baleen is occasionally observed during necropsy examination (Fig. 3), but plate displacement outside the buccal cavity has not been documented in living rorqual or gray whales (although gray whales show asymmetrical wear; Kasuya and Rice, 1970). Bending is presumed to be a post-mortem effect in these taxa. However, misaligned or displaced baleen is occasionally observed in live right whales (Fig. 3), suggesting notable flexibility and range of motion.

Aside from obvious functional concerns for feeding morphology and biomechanics (including stowing in balaenids) plus energetics/metabolism of filtration and drag, the material properties of baleen have implications for mysticete ecology and conservation as they relate to diet, health and toxicology (e.g. pollutant ingestion and interactions with oil). There are major implications for baleen bending with entanglement in fishing gear (van der Hoop et al., 2016; Lysiak et al., 2018), a leading cause of mysticete mortality (Pace et al., 2017). Because whales swim head-first, fishing lines often encircle the rostrum and become enmeshed in the baleen, which adds drag, prevents normal locomotion and affects filtration. The extent to which the baleen 'springs back' to its original position once freed from entanglement may be a major factor for recovery of individual whales or an entire endangered population (Fig. 3).

Our hypothesis-driven study sought to understand whether the baleen is bent when balaenid whales close their mouths and, if so, how it bends. To what extent can different parts of the full baleen filtering apparatus (i.e. the rack) bend? Put simply: how do balaenids stow their baleen? Our comparative analysis investigated several variables: (i) different plates along a rack, from anterior to posterior; (ii) different positions along a plate, from dorsal to ventral and medial to lateral; (iii) different curvatures (i.e. cambering) along a plate; (iv) different environmental conditions (especially air-dried versus hydrated baleen); (v) different baleen components (full plates and/or flat cortical surfaces versus fringes/horn tubes); (vi) different whale species, with baleen of varying size/shape and porosity; (vii) different stages of whale life history, particularly body size and age class.

From a null hypothesis of there being no differences in the variables listed above, we posed an alternative hypothesis that different plates and plate regions, etc., will exhibit differences in flexibility so as to accommodate the filter in a confined space during gape closure.

Manipulation of the jaws of a whale carcass would provide the simplest, most direct means of addressing this question. Unfortunately, this was not possible because of obvious logistical constraints (viz. the size/mass of a whale head). Given the inherent challenges of studying large mysticetes, we synthesized multiple lines of investigation. Our integrative, multifactorial study offered quantitative and qualitative data on baleen flexibility and strength under a wide range of controlled experimental conditions, as follows. (1) Material testing: (i) manual bending of baleen plates to measure pliability and (ii) three-point bending and compression experiments using a materials testing machine. (2) Functional investigation with load cells and kinematic analysis: (i) small-scale experiments with a 90 l circulating flow tank (70-cm-long test chamber) and (ii) large-scale experiments via towing in a 9.84×10^6 l, 245-m-long flow tank. (3) Gross and microscopic morphological examination: (i) histological analysis of the keratin components of baleen and (ii) measurement of the size and density of hollow horn tubes.

MATERIALS AND METHODS

Specimens

Baleen from four species was studied: two balaenids, bowhead (*Balaena mysticetus* Linnaeus 1758) and North Atlantic right whales [*Eubalaena glacialis* (Müller 1776)], and two rorquals (Balaenopteridae), fin [*Balaenoptera physalus* (Linnaeus 1758)] and

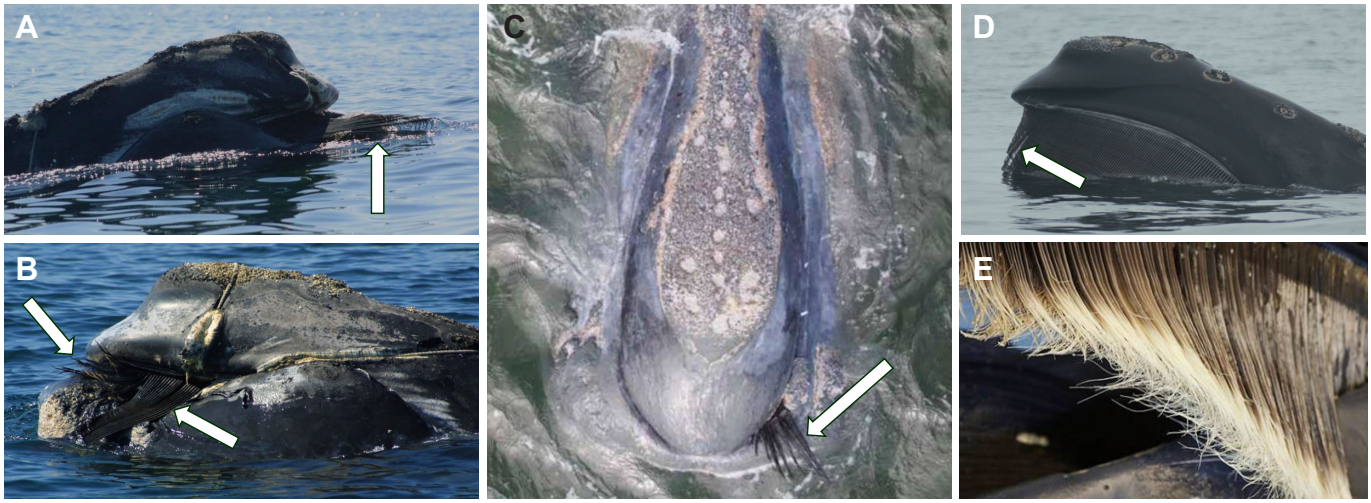

Fig. 3. Baleen misalignment/displacement. The extent to which baleen can bend out of – and back into – its proper position for filter feeding has major conservation consequences for mysticetes, especially highly endangered North Atlantic right whales, *Eubalaena glacialis*, as shown in right (A) and left (B) anterolateral views of the same whale (Eg.2427-2001) with chronic fishing gear entanglement, causing numerous plates to protrude outside the mouth (photo credit: Center for Coastal Studies, NOAA permit 932-1489). (C) Dorsal view of another right whale from an aerial drone (Duke Marine Robotics and Remote Sensing, under permit from NOAA) shows the anterior-most plates protruding, possibly due to entanglement, a major source of whale mortality. (D) Right whales' anterior-most plates are occasionally misaligned or separated from a rack, suggesting plates may move as a result of forces from water flow or anatomical structures (photo credit: M.J.M., NOAA permit 17355-01). (E) Baleen damage has not been documented in live rorquals, but plate shape/position may be altered post-mortem, as here in a juvenile Bryde's whale (*Balaenoptera edeni*) that washed up dead (photo credit: A.J.W.).

humpback whales (*Megaptera novaeangliae* Borowski 1781). No animals were killed or harmed to collect baleen; no baleen was imported from outside the USA. Bowhead baleen was obtained from Inupiat subsistence hunters in Utqiaġvik (Barrow), AK, USA; all other specimens came from animals that died naturally prior to or during stranding in five states along the US Atlantic coast, with collection by the NOAA/NMFS Northeast Marine Mammal Stranding and Disentanglement Network (Virginia, Massachusetts) or NOAA/NMFS Southeast Marine Mammal Stranding Network (North Carolina, Florida, Georgia). Fin whale baleen for histology came from two Eastern Atlantic specimens. All baleen (except bowhead) specimens were frozen until examination, then thawed for testing at room temperature or in chilled water (at temperatures specified below). Full-scale bowhead plates were left attached to gingival tissue, which was soaked in 10% formalin for 7 days to prevent decomposition during shipment and experiments.

Manual bending

For manual bending experiments, a section of 30 full (268–285 cm), adjacent, dried bowhead baleen plates was suspended in normal orientation (distal plate tips hanging ventral-most, with gingiva secured above). Plates were pulled horizontally (anteroposteriorly with respect to the *in vivo* position of the rack) with a Pesola Macro-line spring scale until the plate tip was displaced 45 deg from its original axis, as measured by protractor during bending and confirmed during kinematic analysis via MB-Ruler 5.3 (Markus Bader, Berlin, Germany). Bending was tested at three locations along a dorsoventral axis (near the plate dorsum, middle and ventral tip) in three plates along a rack's anteroposterior axis (with cranial, central and caudal plates). Plates were pulled on the medial (fringed) side and again from the lateral side. These axial bending tests were repeated with the same plates in the normal hydrated condition (kept for 14 days in 12°C artificial seawater that was circulated to avoid surface biofilm formation or tissue degradation). Dry/wet tests were repeated on a section of humpback baleen (16 adjacent plates, 53–57 cm long); again, angles were measured via protractor and MB-Ruler 5.3.

Mechanical testing

For mechanical strength testing, right whale baleen was cut into 50, 3×3 cm squares using a band saw. All squares were cut from the midline of the mediolateral axis (i.e. between the lingual and labial sides). The thickness of the tissue squares was almost perfectly uniform (mean±s.d. 2.87±0.03 mm, range 2.82–2.95 mm, N=50). Half of the square samples were kept in air and half were placed in flowing seawater at 12°C for 21 days. The samples were transported in air or water until just prior to testing on an Instron E1000 ElectroPuls universal testing machine (Instron/ITW Corp., Norwood, MA, USA) or Mark-10 ES30 universal testing machine with M4-200 force gauge (Mark-10 Corp., Copiague, NY, USA). To investigate the tissue's compressive strength via a three-point bending test, the small wet or dry baleen samples were placed on two arms spaced slightly apart: 18.92 mm for Instron testing and 24 mm for Mark-10 testing. Samples were oriented so the direction of internal horn tubes was perpendicular to the arms on which samples rested. The materials testing device recorded the force and resulting strain, including the maximal force encountered by each tissue sample before failure or before the machine reached its displacement limits, which occurred often with hydrated samples.

Using the thickness and other dimensions of the square samples, and the distance between the points on which the samples lay, the flexural stress and strain were computed for each trial. From these values, the flexural stiffness (a function of the modulus) could also be determined for each trial. Because the stress–strain curves were not linear, flexural stiffness was defined as the largest slope regressed using a continuous subset with size 25% of the original data (Patek et al., 2013). All initial tests were performed with the Instron machine. These were repeated (with 40 additional baleen samples from the same individual right whale) with the Mark-10 testing machine. All tests on three control materials (3×3 cm squares of aluminium, HDPE plastic, lauan plywood) were also performed with the Mark-10 machine. Because our analysis uses a baleen dataset with pooled data from the two machines, statistical ANOVA tests were performed to compare results from the Instron versus Mark-10 testing. The same slope-finding algorithm (Patek et al., 2013) was used to determine flexural stiffness on data obtained from the two machines. Both manual and machine bending tests were repeated with wet/dry samples of humpback baleen.

Functional (flow tank) experiments

Small-scale functional testing was conducted with artificial seawater in a 90 l circulating flow tank made of PVC in a vertical loop, modeled on a design by Vogel (1996), with an acrylic viewing port through which a ruled grid could be seen behind the test chamber (70 cm long, 900 mm^2 cross-sectional area). Cut sections (20 cm long×7 cm wide) of dried or wet right, bowhead and humpback baleen were clamped to a metal rod in groups of six, oriented transversely (normal position as *in vivo*, 90 deg to water flow) and spaced 1 cm apart, then submerged in water flowing at 5–140 cm s^{-1} (following Werth, 2013). Lateral kinematic sequences were videotaped from the viewing window and underwater from the testing chamber in anterior view with an illuminated digital endoscope (5/25/50 cm focal distances; VideoFlex SD, Umarex-Laserliner, Arnsberg, Germany) that recorded JPEG images and AVI video (30 frames s^{-1}).

Large-scale testing was conducted at the Oil and Hazardous Materials Simulated Environmental Test Tank (OHMSETT) National Oil Spill Response Facility at Naval Weapons Station Earle in Leonardo, NJ, USA. This above-ground concrete tank filled with 9.84×10^6 l (2.6×10^6 gallons) of seawater measures 245 m long, 20 m wide and 2.6 m deep, with a wave generator and mobile towing bridge. Seven 'mini-racks' of 15–30 full-size bowhead plates 2.5–3 m long (exclusive of gingiva) were clamped to a turntable and rotated 54 deg (to simulate proper orientation within intraoral incurrent flow) or 90 deg (flow perpendicular to plate transverse orientation), then towed at 0.2–1.6 knots (0.36–3 km h^{-1} or 0.1–0.82 m s^{-1}) as a 445 N or 2224 N Omega load cell between the baleen and turntable recorded drag forces (following Cavatorta et al., 2005). Because mini-racks were towed with no features simulating whales' lips or other surrounding structures, in some trials proximal (near-gum) portions of baleen plates were tied with monofilament line to keep the spacing (~1 cm) of the distal plate sections the same as at the gingiva. Trials with full-length right and humpback whale plates were also conducted. Trials were documented via underwater video-recording, along with photo/video-recording from the surface and underwater viewports.

For both the small- and large-scale flow trials, still photographs or video frames were analyzed with ImageJ; kinematic sequences were viewed frame-by-frame via GoPro Studio v.2.5.7, with landmarks digitized via Tracker v.4.92 and MB-Ruler 5.3 to quantify angle of bending (Fig. 4).

Histological examination

For histological study, samples of bowhead and fin whale baleen, from gingival emergence at the Zwischensubstanz (Pinto and Shadwick, 2013) to the ventral tip, were embedded, stained

Journal of Experimental Biology (2018) 221, jeb189233. doi:10.1242/jeb.189233

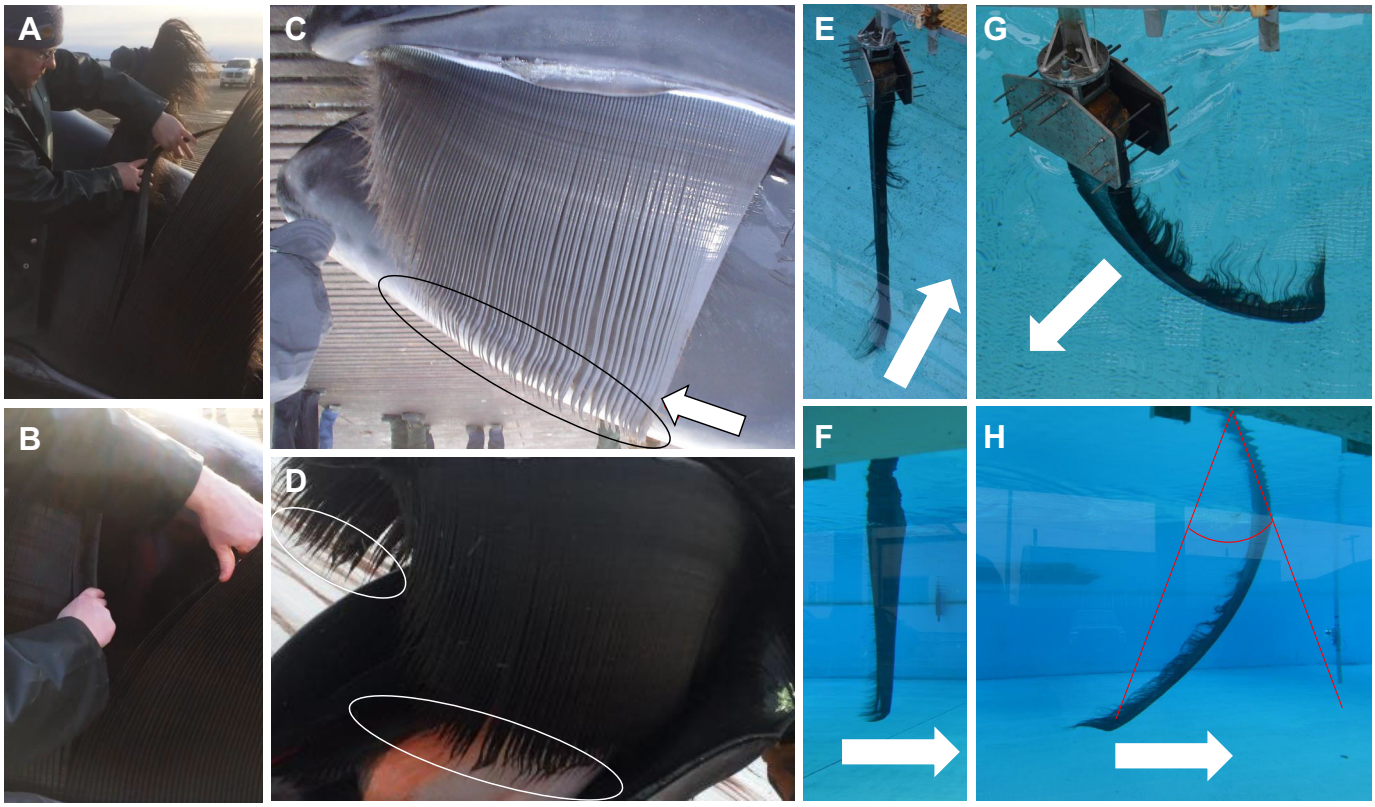

Fig. 4. Manual and flow-induced bending. (A,B) Manual bending of wet baleen in a recently landed bowhead shows high flexibility of individual plates (A) and large sections of adjacent plates (B). (C,D) These photos of recently landed bowheads show bent ventral-most plate tips (circled); arrow in C shows the 'natal notch', above which baleen is grown after birth. (E–H) Bending of 'mini-racks' of 30 full-size bowhead baleen plates towed (in the direction of the white arrows) in a large flow tank at 0.4 m s^{-1} (E,F) and 1.2 m s^{-1} (G,H). Note, there is fringe movement at all speeds but plate bending only at high speed (seen above the surface in E and G and via the underwater viewport in F and H). Image H indicates how plate tip bending angle (divergence from original straight axis) was obtained from the photographs. Photo credits: T.L.S. (A–D); A.J.W. (E–H).

(Mallory trichrome and hematoxylin–eosin), sectioned, and examined via microscopy, paying attention to the thickness of cortical keratin sheets relative to interior keratinous structures (hair-like, cylindrical horn tubes and intertubular horn cells; Fudge et al., 2009). Horn tube analysis allowed comparative quantification of histological differences within and between baleen plates. Widths of cortical and medullary regions were compared, as were horn tube external and internal (luminal) diameter and the density of tubes per unit area.

RESULTS

Manual bending

Results of the axial bending tests (Fig. 5) confirm that hydrated right whale baleen is significantly (P=0.02 via t-test, N=180) more flexible than dried baleen, with forces needed to bend the baleen 45 deg from its original vertical axis averaging 10.33±1.98 N in hydrated baleen (mean±s.d., range 7.6–13.1 N, N=180) versus 38.46±8.46 N in dried baleen (range 26.3–52.1 N, N=180). Overall, dried baleen required a mean (±s.d.) of 3.77±0.67 times more force

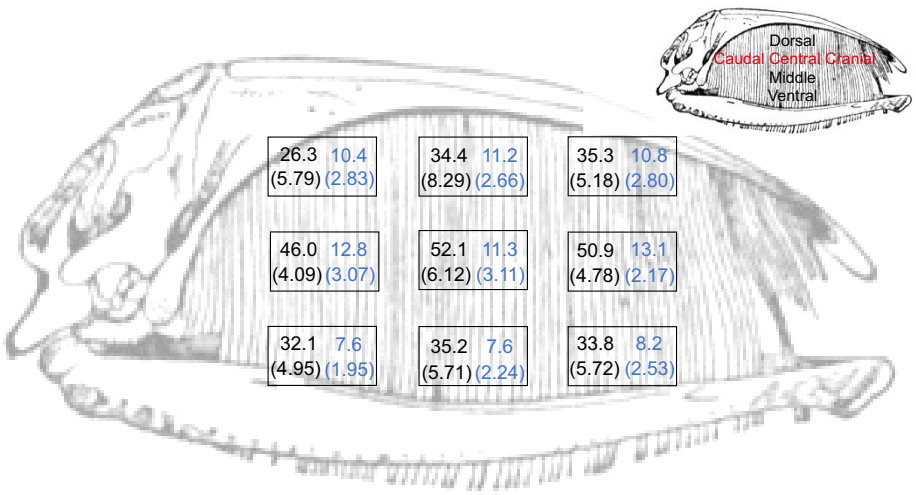

Fig. 5. Manual bending results. Mean (and s.d. in parentheses) force (in N) from 20 experimental trials, producing 45 deg axial bending in air-dried and hydrated (black and blue numbers, respectively) bowhead whale plates, indicating differences in nine locations along the dorsoventral and anteroposterior axes.

Journal of Experimental Biology (2018) 221, jeb189233. doi:10.1242/jeb.189233

to achieve the same degree of bending. However, regional differences in bending were less apparent. There was a slight trend toward increased flexibility in moving from the anterior to the posterior of a rack (with 40.0 N needed anteriorly to achieve the same baleen flexion as 34.8 N posteriorly), but mostly this difference was not statistically significant (P=0.44, N=360), depending on dorsoventral position. However, there was a clearer increase in flexibility of dorsal and ventral baleen relative to the midline portion of a plate's dorsoventral axis (throughout the anteroposterior range of a rack; Fig. 5). Dorsal baleen was bent 45 deg with a mean (±s.d.) of 32±4.04 N (N=60) and ventral baleen was bent 45 deg with a mean of 33.7±1.27 N (N=60) versus a mean (±s.d.) of 49.7±2.63 N (N=60) for baleen in the middle of a plate's vertical axis. These findings hold in both air-dried as well as wet baleen, but ventral-most tips bent especially easily when hydrated (Fig. 4C,D). ANOVA testing revealed slight significance (P=0.047, N=180) for these dorsoventral differences. In terms of mediolateral differences, plates were slightly yet not significantly (P=0.14, N=180) more flexible when bent from the lateral (labial) side instead of the medial (lingual) side, even though the lateral edge often has a cambered foil-type curve that is absent medially. Lateral portions bent 45 deg with a mean (±s.d.) of 27.43±3.76 N (range 19.2–34.4 N, N=180) versus 36.8±3.22 N for the medial edge (range 24.9–42.1 N, N=180).

Mechanical testing

Mechanical strength testing likewise revealed substantial and significant (P=0.02, N=50) differences in the material properties of dried versus hydrated right whale baleen, regardless of location along a plate or within a rack (Figs 6 and 7). Dried baleen cracked and failed – shattering into small pieces – under high stress (at about 500 N; mean±s.d. 488.3±11.4 N, range 467.7–581.2 N, N=25) but with little displacement (strain <2 mm; mean±s.d. 1.67±0.06 mm, range 1.59–1.82 mm, N=25), whereas wet baleen bent easily (high strain) with minimal stress. Wet baleen absorbed over 1 kN (mean ±s.d. 1294.6±42.3 N, range 1094.4–1636.8 N, N=25) of force before the machine reached the upper limit of its range of measurement (30 mm displacement). Wet samples displayed elasticity, rebounding to their original form without failure. Although there was much variation (Fig. 7A), baleen in the middle of a plate, whether wet or dry, absorbed more stress (mean ±s.d. 1.83±0.46 times, range 0.88–2.27 times, P=0.11, N=50) before failing/maxing out relative to baleen closer to the tip or dorsum. The flexural stiffness or modulus (the slope of the stress–strain curve) was also far greater (mean±s.d. 6.75±0.82 times, range 4.12–10.33 times, P=0.04, N=50) in dried relative to hydrated baleen, and was often higher in the middle or dorsal sections of a plate, although this was not always the case (Fig. 7B). As with measurements of maximum stress, flexural stiffness exhibited differences along a rack's anteroposterior axis (i.e. in plates from the cranial, central and caudal regions), but without any discernible or statistically significant (P=0.21, N=50) pattern (Fig. 7). Manual axial bending and materials strength (3-point bending) tests were repeated with full plates and sample squares of humpback baleen. Once again, baleen that was kept in water for >6 days was much more flexible (mean±s.d. 3.77±0.18 times, range 2.94–3.98 times, P=0.05, N=50) than air-dried baleen; however, no significant differences (P=0.17, N=50) were observed in terms of flexibility along a plate or rack. Fin and humpback whale baleen did not show significant differences from each other in tests of mechanical strength (P=0.32, N=44), but together (with results pooled), data indicate that the baleen of these rorqual species is significantly (P=0.49, N=44) less flexible than that of right whales when both are hydrated (maximum stress before failure: mean±s.d. 382.6±23.9 N, range 344.7–422.7 N, N=44) and air-dried (767.4±34.3 N, range 612.1–872.0 N, N=44). No mechanical differences were noted for fin and humpback whale baleen in terms of dorsoventral location along plates.

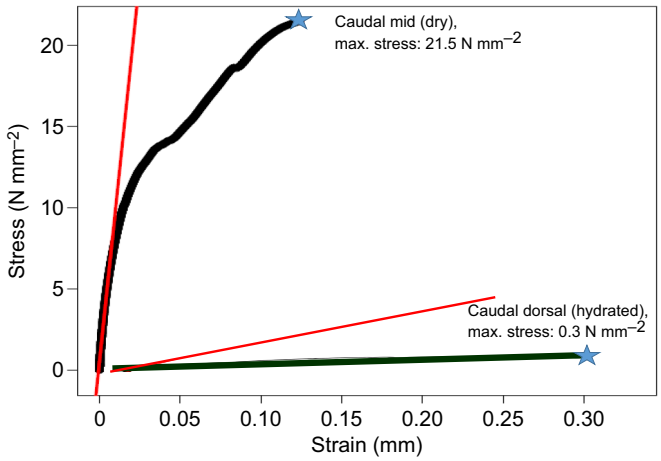

Fig. 6. Mechanical testing results. Maximal stress recorded from 3-point bending tests of air-dried and hydrated right whale baleen plate samples shows noodle-like flexibility of wet baleen and brittle fracturing of dry baleen, which failed at 12 mm displacement (=strain).

Functional (flow tank) experiments

Small-scale functional (flow tank/flume) testing of bowhead, right and humpback whale baleen plate sections did not provide conclusive findings with regard to varying flexibility along any directional axis (dorsoventral, anteroposterior or mediolateral). Baleen kept hydrated for >6 days prior to flow testing was considerably more flexible than dried baleen (mean±s.d. 212±13%, range 61–234%, P=0.03, N=40) based on bending angle from photographs/video frames. Perhaps because all plate sections were small (7×20 cm), no significant differences were observed by species (P=0.14, N=36), except that the longer fringes of bowhead/right whale baleen moved to the plate's trailing edge even at low flow speeds (5–10 cm s^{-1}); the plates themselves displayed little bending.

In contrast, the large-scale tow testing of 15– 30 full (2.5–3 m) bowhead plates revealed differences in bending whether viewed from above the surface or underwater (Fig. 4). In quantitative terms, with bending angle determined via ImageJ and MB-Ruler 5.3 analysis of photographs and video frames (Fig. 4), full-size plates showed a mostly linear increase in bending with flow speed (Fig. 8), though with little (<10 deg, mean±s.d. 6.56±0.23 deg, range 4.88–8.92 deg, N=18) bending at low flow speed (0.2–0.4 m s^{-1}). At a flow of ~0.4 m s^{-1}, bending angle jumped to nearly 20 deg and rose steadily until flow speed exceeded 1 m s^{-1}, where the angle held steady at about 37 deg (mean±s.d. 37.44±0.36 deg, range 36.91–37.89 deg, N=18; Fig. 8). In qualitative terms, a similar relationship between tow (=water flow) speed and baleen bending was observed (Fig. 4); at the lowest speeds, the plates themselves remained straight, with only the fine, free fringes trailing behind (Fig. 4). As flow speed increased, the plate began to bend, first with the lower third of the plate(s) bending away from the direction of flow (at ~0.6 m s^{-1}; Fig. 4G), then with the upper third bending similarly when flow reached or exceeded 1 m s^{-1} (Fig. 4H). The plate midline appeared to remain straighter than the dorsal- and ventral-most baleen.

Journal of Experimental Biology (2018) 221, jeb189233. doi:10.1242/jeb.189233

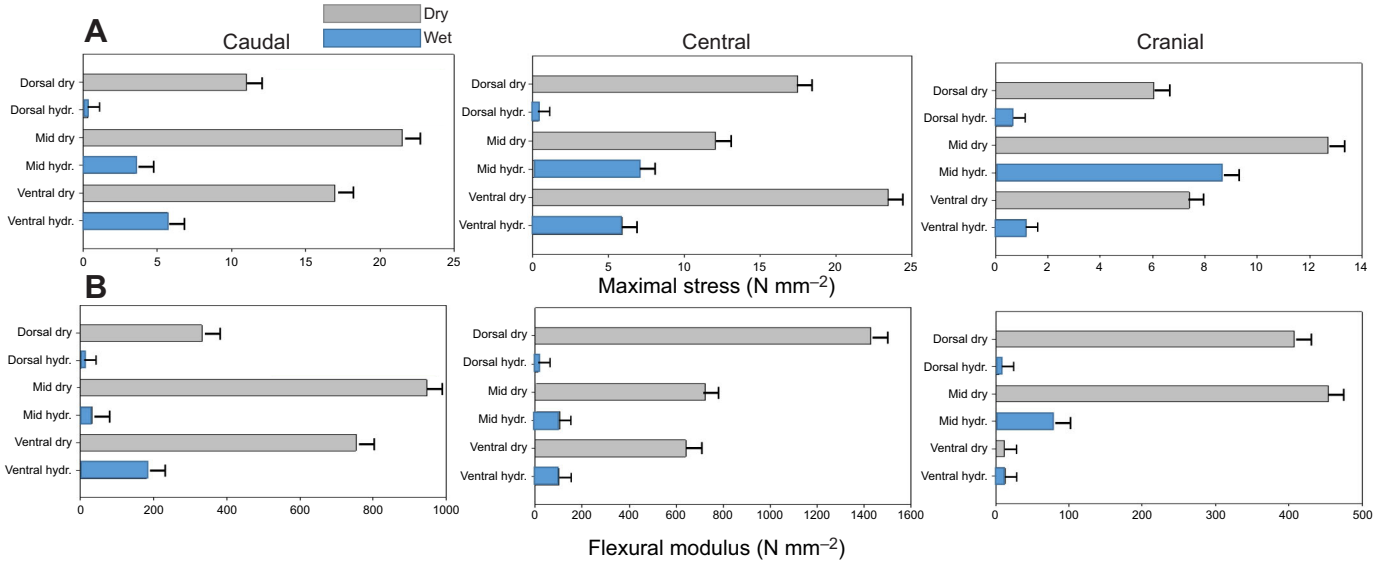

Fig. 7. Maximal stress and flexural stiffness according to location along the plate. Maximal stress (A) and flexural modulus (=stiffness, B) from material strength testing of air-dried (gray bars) versus hydrated (blue bars) right whale baleen samples, showing data from nine locations along the anteroposterior and dorsoventral axes.

As expected, load cells indicated a linear increase in drag as water flow/tow speed increased. There was no discernible or significant (P=0.27, N=34) variation in the anterior- versus posterior-most plates (i.e. on the leading/trailing edges of a mini-rack) in terms of the degree of bending (Fig. 4). Plates bent solely in the posterior direction. Limited right whale trials revealed bending similar to that of bowhead whale baleen; humpback whale baleen showed a slight posterior flexion (<20 deg) only at high tow speeds (>1 m s^{-1}), with nearly all flexion in the lower (distal) third of plates.

Histological examination

Histological examination of baleen from bowhead and fin whales revealed significant, substantial differences in both species along the mediolateral axis of a plate, with horn tubules on a plate's lateral (labial) side being far less abundant, but with a larger diameter externally and especially of the hollow central lumen, relative to a plate's medial side adjacent to the tongue (Fig. 9). Horn tubule density on the lateral side of baleen plates averaged 1.92±0.24 mm^{-2} (mean±s.d., range 1.83–2.22 mm^{-2}, N=40) in bowhead whales and 1.64±0.38 mm^{-2} (range 1.03–2.49 mm^{-2}, N=28) in fin whales, versus 3.21±0.37 mm^{-2} (range 2.79–3.46 mm^{-2}, N=40) for the medial side in bowhead whales and 3.84±0.67 mm^{-2} (range 2.23–4.89 mm^{-2}, N=27) in fin whales. In terms of size, horn tubules on the lateral side of baleen plates averaged 2093.3±40.1 µm (mean±s.d., range 512.2–2440.8 µm, N=40) in bowhead whales and 2168.2±76.1 µm (range 472–2583 µm, N=28) in fin whales, versus 189.0±22.2 µm (range 45.9–378.6 µm, N=40) for the medial side in bowhead whales and 283.0±41.5 µm (range 38.2–456.3 µm, N=27) in fin whales. These represent significant differences in both tubule density (P=0.02, N=28) and size (P=0.03, N=28) between lateral and medial plate regions. Baleen of fin whales had up to 300% more tubules on the medial side than on the lateral/labial side (Fig. 10A), and in bowhead whales, medial baleen had 60–105% more tubules per mm^2 than lateral baleen. The cortical or flat outer region of the baleen (without horn tubules or intertubular keratin) was much thicker laterally (Fig. 9AB) relative to the medial baleen (Fig. 9C, D), with cortical thickness of the lateral side averaging 683 µm in bowhead whales and 978 µm in fin whales versus 244 µm for the lingual side in bowhead whales and 212 µm in fin whales. Plates were also thinner overall (including both tubular medullary and flat cortical baleen) medially relative to the lateral side (mean±s.d. 2.4±0.15 mm, range 2.22–2.93 mm, N=40 versus 3.3±0.18 mm, range 2.45–3.79 mm, N=40, for bowhead whale medial and lateral sides, respectively; P=0.05). Plates were thinner distally relative to their proximal (dorsal) gingival origin (mean±s.d. 1.92±0.22 mm, range 1.77–2.45 mm, N=40 versus mean±s.d. 3.44±0.29 mm, range 2.46–3.75 mm, N=40, for bowhead whale distal and proximal regions, respectively; P=0.03).

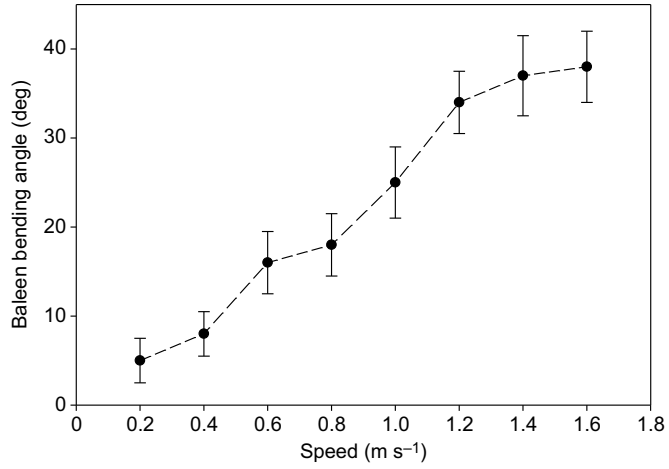

Fig. 8. Angle of bending (±s.d.) versus water flow (=tow) speed for 'mini-racks' of 30 full-size bowhead whale baleen plates.

DISCUSSION

Our findings support the conclusions of previously published research, especially the pronounced difference between dried and hydrated baleen tissue (Werth et al., 2016a) and flow-induced entanglement of fringes to create a mat-like mesh (Werth, 2013). However, the bending of baleen plates has not previously been the

Journal of Experimental Biology (2018) 221, jeb189233. doi:10.1242/jeb.189233

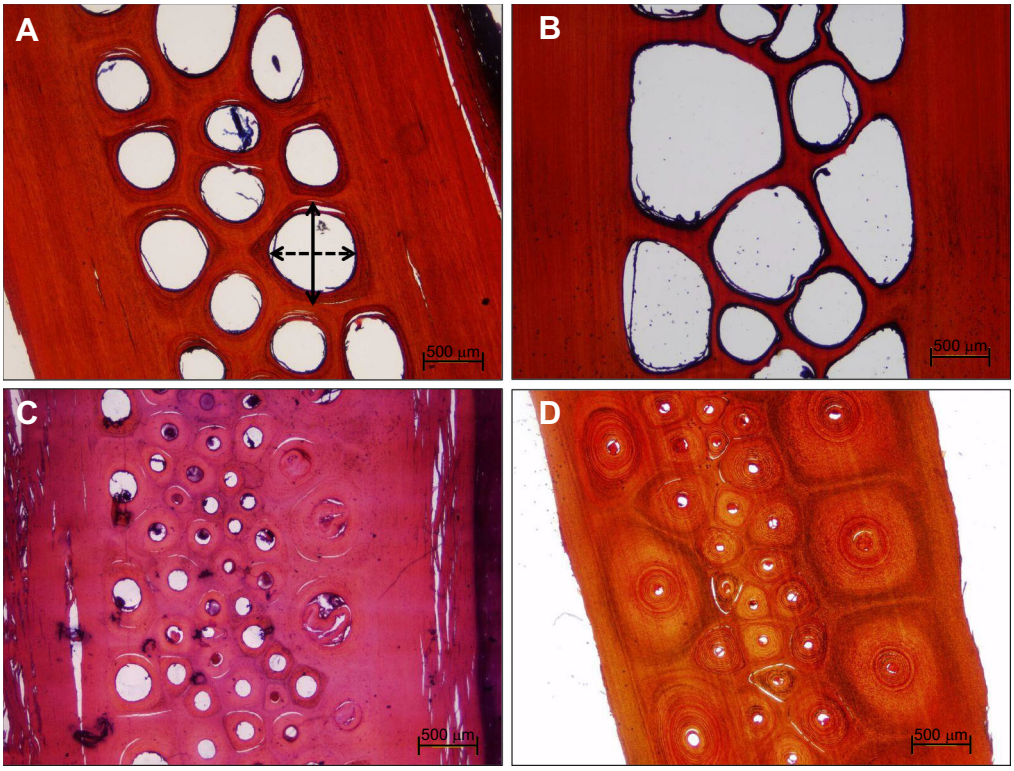

Fig. 9. Tubular ultrastructure of baleen. Close-up views of transversely sectioned fin whale baleen (A,C: plate no. 81; B,D: plate no. 97) showing large-diameter hollow horn tubules (medullary lumen 500–2500 µm) in the lateral/labial region of the plate (A,B) versus much narrower (40–400 µm) yet more numerous tubules in the plate's medial/lingual region (C,D). In A, the solid arrow indicates the external tubular diameter; the dashed arrow shows the diameter of the hollow lumen.

subject of focused biomechanical investigation or experiment, despite published speculation (Gray, 1877). Our integrative study of baleen bending revealed a complex story, not only because multiple factors independently and collectively govern plate flexibility and mobility (including dorsoventral, mediolateral and anteroposterior positions) but also because additional (potentially confounding or complicating) factors directly or indirectly contribute to stiffness/flexibility. Among these are gross anatomy, baleen plate geometry, life history and function, as detailed below.

Gross anatomy: dorsal-most baleen is fixed in position (where it emerges from the gumline proximally) whereas the free distal tip is farthest from this attachment.

Baleen plate geometry: each plate can be simplified as a scalene triangle, widest (mediolaterally) dorsally and narrowest at its distal tip, which complicates dorsoventral comparison of flexibility.

Life history: the dorsal-most (proximal) baleen is youngest (newest), whereas the distal tip has the oldest baleen. Also, older whales have longer baleen; shorter juvenile/subadult baleen may not be fully hardened. Calcification likely plays a role in baleen stiffness (Szewciw et al., 2010), with calcium salt crystals deposited during baleen formation. Hence, new baleen at the gumline is probably the softest, whereas older (more distal) baleen has crystals that have hardened. Middle sections of baleen have had time to harden but not yet erode substantially (i.e. as much as the tip) and

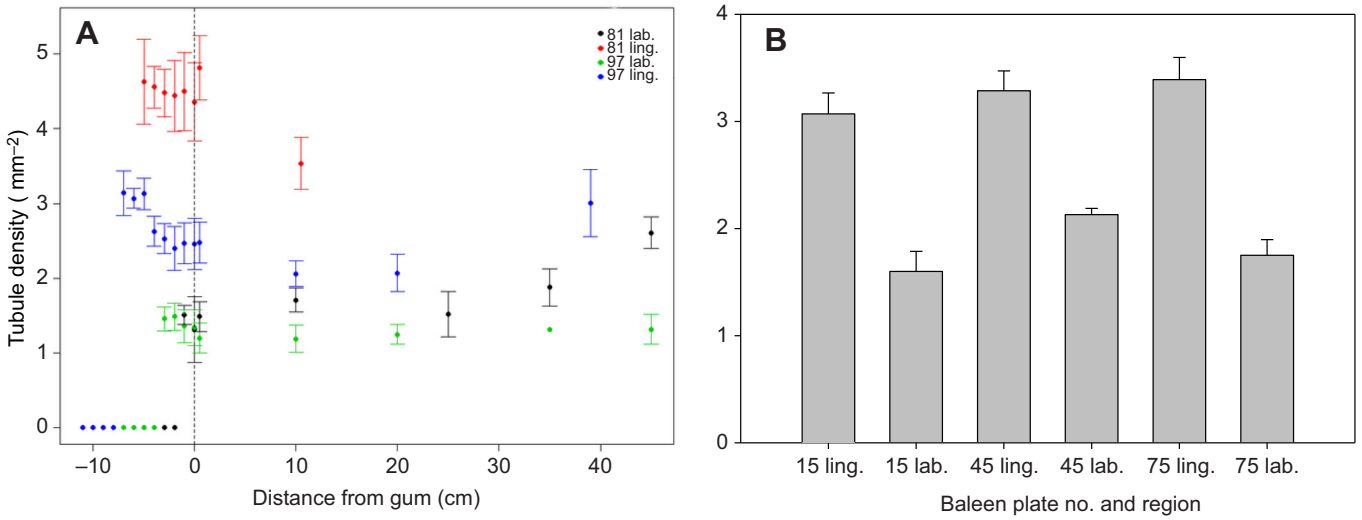

Fig. 10. Comparative tubular density. Density of hollow horn tubules (means±s.d.) in fin whale (A, based on two plates) versus bowhead whale (B, three plates) baleen, showing greater density in the lingual (medial) region of the baleen than in the labial region for both species.

lose structural integrity or stiffening crystals as a result of wear (Werth et al., 2016b).

Function: baleen is least worn dorsally and most worn – from friction of food items (Werth, 2012), flowing water (Werth, 2013) and contact with anatomical structures (the tongue, lips, adjacent plates, etc.; Werth, 2001) – at the distal tip.

Altogether, dorsal-most baleen is newest, widest, thickest, least worn and fixed in place; baleen at the free ventral tip is oldest, narrowest, thinnest and most worn, with most horn tubes fully or partially exposed as hair-like fringes (Pfeiffer, 1992). Because of its intermediate age and wear (and other factors outlined above, including hardening of calcium crystals deposited as baleen forms and emerges from the gingiva; Szewciw et al., 2010), baleen in the middle of a plate may be the strongest. Slight transverse growth ridges (Ruud, 1940), similar to those found in human fingernails (Forslind, 1970), appear not to affect mechanical strength or resistance to erosion. However, these ridges (undergoing further investigation) appear to reflect faster medial growth, potentially affecting flexibility.

Overall, baleen of bowhead and right whales is very strong (absorbing over 1 kN of force in our tests) and highly flexible, especially when wet and where thinnest. Loading (deformation) curves (i.e. stress–strain plots; Fig. 6) reveal the elastic nature of baleen, with all tested samples that did not fail – which occurred only with unrealistically dried baleen – returning to their normal shape/position after loading.

Returning to our operational hypothesis, it is difficult to provide a definitive answer to the question with which we framed this study (viz. how do balaenids stow their baleen?). However, it is clear that baleen flexibility varies by location according to the multifactorial variables outlined above (and perhaps others). Multiple lines of experimental and observational evidence suggest baleen plates bend mostly evenly along their length but may be slightly more flexible dorsally (where newer and softer) and ventrally (where plates are narrower, thinner, more worn and farthest from their attachment to the palate). There appears to be much more medial than lateral wearing. Plates are not 'hinged' where they emerge from the gums. Along a rack's anteroposterior axis, there appear to be no key differences, although central plates are longer and slightly thicker, possibly making them less flexible. The most anterior and posterior plates are shortest and possibly experience the greatest loading (from incurrent water flow and contact with tissue at the posterior extent of the buccal cavity, respectively), possibly leading them to be more flexible, and potentially explaining why these plates may be pushed 'out of alignment' (Fig. 3A,B) or more likely to be deformed by rope entanglement, as is occasionally observed (Dolman and Moore, 2017).

Although plates are unlikely to flex along their mediolateral axis because of their wide span, the lateral edge is, as a result of its greater density of wide, hollow horn tubes, more likely to flex than the medial side, where the baleen meets the tongue (although the lateral baleen is thicker, with a wider region of flat cortical keratin). Variation in tubular size and density may explain why plates flex more readily on lateral (relative to medial) sides in manual axial flexion tests. Preliminary evaluation of baleen orientation in bowhead whales hauled out on ice after subsistence hunting suggested plates might curl medially, toward and perhaps under the tongue (Fig. 4), to accommodate their extreme length during gape closure. However, the greater baleen medial stiffness (due to smaller, denser horn tubules) relative to lateral stiffness makes this unlikely. Increased stiffness along the baleen lingual surface may impede medial erosion (from the tongue, prey or water). Increased labial flexibility may better allow the filter to expand during gape opening, to accommodate and dissipate forces from continuous water flow or to improve filtration. The latter explanation is unlikely, however; even if an expanded filter has a higher surface area, this comes at the expense of greater porosity (St Aubin et al., 1984; Mayo et al., 2001; Werth, 2013), which might hinder balaenid foraging. Further, the apparent curling of the baleen under the tongue may be an artifact created when highly flexible distal tips (mostly matted fringes with little flat cortical keratin) are bent as whales are repositioned post-mortem. Alternatively, this may represent the so-called natal notch separating postnatal baleen from baleen grown *in utero* (Schell et al., 1989), which typically appears as a bend (Fig. 4C).

The cambered curve of bowhead/right whale baleen (entirely absent or barely detectable in other mysticete species; Werth and Potvin, 2016) may relate to flexibility, possibly by stiffening plates the way corrugations of cardboard or metal resist flexion. Balaenid baleen is notably curved posteriorly on its lateral edge (about 24 deg off axis; Werth and Potvin, 2016), which, according to standard beam theory, would increase stiffness. Decreased flexibility would seem to work against the hypothesis of enhanced flexibility needed for balaenids to stow their unused filter in the closed mouth, which suggests the filter might be sufficiently flexible, especially when fully expanded and subjected to flowing (dense, viscous) water to require longitudinal stiffening. Alternatively, this hydrofoil-like cross-section may improve continuous water flow (resisting drag or even generating lift; Potvin and Werth, 2017) to aid prey capture. At the same time, cambering may reduce lateral flexibility to keep the filter from expanding, which would impede filtration.

Overall, right and bowhead whale filters are probably easily stowed because their baleen tissue, when hydrated (in life), is highly flexible. The results suggest plates/racks likely bend mostly evenly along their length. Attempts to bend whole baleen attached to the palate *in situ* (in whale carcasses on land; Figs 1C,D and 4A,B) proved unsatisfactory. Even if a whale's body/mouth lies in its normal orientation, the baleen is unsupported by water buoyancy and instead is influenced by gravity. In the absence of data recorded *in vivo* (e.g. from telemetric or archival tags attached to the baleen), controlled experiments offer the best alternative, particularly when – as here – they involve varied structural and functional considerations in an attempt to replicate real-life conditions.

The flow speeds at which our tests/observations indicated the greatest changes in bending (i.e. 0.8–1.2 m s^{-1}; Fig. 7) correspond with shipboard observation and biologging tag data of feeding bowheads, namely 0.8–1.0 m s^{-1} (Simon et al., 2009; Goldbogen et al., 2017), suggesting that balaenid whales might forage at speeds just at the limit of where their baleen begins to bend, which would potentially enlarge or otherwise alter filter porosity (Werth, 2013). Alternatively and perhaps more likely, the bending properties of balaenid baleen may have adapted to suit ideal foraging speeds, which may relate to drag incursion or prey sensing/dispersal. Despite this apparent similarity, swimming and test speeds could in fact differ because an internal pressure head (from the medial mat of tangled fringes) would likely result in lower ram filtration flow rates than a whale's locomotor speed.

Like other mysticetes, balaenids likely undergo prolonged periods of winter fasting (when on mating/calving grounds), but even if the mouth is normally closed for extended periods, their baleen shows no indication of remaining bent once the mouth opens. This suggests plates retain sufficient flexibility to resume full extension when gape widens. Of course, the mouth may be opened frequently year-round, perhaps for thermoregulation via a palatal rete (Ford et al., 2013), or even for winter feeding (Aguilar et al., 2014; Pomerleau et al., 2018). The audible 'baleen rattle' during balaenid surface skim feeding (Watkins and Schevill, 1976) represents the clacking of adjacent baleen, indicating that plates

are flexible enough to touch each other but strong and straight enough to spring back to their default orientation, separated by a 1 cm inter-baleen gap (Werth and Potvin, 2016).

Overall, rorqual baleen shows similar strength and hydration effects as that in balaenids, but with lower flexibility and no apparent differences by plate region. Hydrated baleen plates of all mysticete species are not only flexible but also especially strong in compression. Fringes are tough, pliable and ductile; they resist compression, tension and bending, which likely aids in ensuring that fringes are not pushed out of position (Werth and Ito, 2017) or abraded and eroded away (Werth et al., 2016b) during filtration or gape closure. Ongoing research on simulated (3D-scanned and printed) baleen with variable stiffness and other material properties will allow biomimetic exploration but also experimentation beyond the parameters of naturally occurring whale tissue.

Acknowledgements

This project was inspired by John Gosline and Steve Vogel. We thank the Alaska Eskimo Whaling Commission and Barrow Whaling Captain's Association, especially Billy Adams, Harry Brower, Jr, and Qaiyaan Harcharek for providing bowhead baleen; Tom Pitchford, Bill McLellan, Kristján Loftsson and Erin Fougeres gave access to other specimens. Scott Landry (Center for Coastal Studies) and Dave Johnston (Duke University) provided field photos. Research was conducted under NMFS Permits 17350 and 18786, with help and approval from the NOAA Office of Response and Restoration/Emergency Response Division (Gary Shigenaka), NOAA/NMFS Marine Mammal Health and Stranding Response Program (Teri Rowles) and OHMSETT (Alan Guarino). Many scientists aided this project through lab/field assistance (Craig George, Tom Lanagan, Jason Kapit, Geof Givens, Sheila Patek) or discussions/ideas, including Bob Shadwick, Jeremy Goldbogen, Jean Potvin, Nick Pyenson, Frank Fish, Chris Marshall, Joy Reidenberg, Tom Ford, Stormy Mayo and Amy Knowlton. Two anonymous reviewers provided valuable suggestions that improved the final manuscript.

Competing interests

The authors declare no competing or financial interests.

Author contributions

Conceptualization: A.J.W.; Methodology: A.J.W., D.R., M.V.R., M.J.M., T.L.S.; Software: A.J.W., M.V.R.; Validation: A.J.W., M.J.M., T.L.S.; Formal analysis: A.J.W., M.J.M., T.L.S.; Investigation: A.J.W., D.R., M.V.R., M.J.M., T.L.S.; Resources: A.J.W., D.R., M.V.R., M.J.M., T.L.S.; Data curation: A.J.W., D.R., T.L.S.; Writing - original draft: A.J.W.; Writing - review & editing: A.J.W., D.R., M.V.R., M.J.M., T.L.S.; Visualization: A.J.W., D.R., M.V.R., T.L.S.; Supervision: A.J.W.; Project administration: A.J.W., T.L.S.; Funding acquisition: A.J.W., T.L.S.

Funding

Funding for A.J.W. came from Hampden-Sydney College faculty grants and a Harris Award from the Virginia Foundation for Independent Colleges. National Oceanic and Atmospheric Administration CINAR Award NA14OAR4320158 and North Slope Borough, Alaska, funded OHMSETT testing.

Data availability

All data are freely available in the Dryad Digital Repository (Werth et al., 2018): dryad.73rm81p.

References

Aguilar, A., Giménez, J., Gómez-Campos, E., Cardona, L. and Borrell, A. (2014). δ^{15}N value does not reflect fasting in mysticetes. *PLoS ONE* **9**, e92288.

Bengtson, J. L. and Stewart, B. S. (2018). Crabeater seal, Lobodon carchinophaga. In *Encyclopedia of Marine Mammals 3e* (ed. B. Wursig J.G.M. Thewissen and K.M. Kovacs), pp. 230-232. San Diego: Academic Press.

Bertram, J. E. A. and Gosline, J. M. (1986). Fracture toughness design in horse hoof keratin. *J Exp. Biol.* **125**, 29-47.

Bertram, J. E. A. and Gosline, J. M. (1987). Functional design of horse hoof keratin: the modulation of mechanical properties through hydration effects. *J. Exp. Biol.* **130**, 121-136.

Best, P. B. and Schell, D. M. (1996). Stable isotopes in southern right whale (Eubalaena australis) baleen as indicators of seasonal movements, feeding and growth. *Mar. Biol.* **124**, 483-494.

Caraveo-Patiño, J., Hobson, K. A. and Soto, L. A. (2007). Feeding ecology of gray whales inferred from stable-carbon and nitrogen isotopic analysis of baleen plates. *Hydrobiologia* **586**, 17-25.

Cavatorta, D., Starczak, V., Prada, K. and Moore, M. J. (2005). A note on the friction of different ropes in right whale baleen: an entanglement model. *J. Cet. Res. Mgmt.* **7**, 39-42.

Dolman, S. J. and Moore, M. J. (2017). Welfare implications of cetacean bycatch and entanglements. In *Marine Mammal Welfare* (ed. A. Butterworth), pp. 41-65. New York: Springer.

Eisenmann, P., Fry, B., Holyoake, C., Coughran, D., Nicol, S. and Bengtson Nash, S. (2016). Isotopic evidence of a wide spectrum of feeding strategies in Southern Hemisphere humpback whale baleen records. *PLoS ONE* **11**, e0156698.

Feughelman, M. (1997). The relation between the mechanical properties of wool and hair fibres and the keratin-water system. In *Mechanical Properties and Structure of Alpha-Keratin Fibres* (ed. M. Feughelman), pp. 16-27. Sydney: Univ. of New South Wales Press.

Feughelman, M. (2002). Natural protein fibers. *J. Appl. Polym. Sci.* **83**, 489-507.

Ford, T. J., Werth, A. J. and George, J. C. (2013). An intraoral thermoregulatory organ in the bowhead whale (*Balaena mysticetus*), the corpus cavernosum maxillaris. *Anat. Rec.* **296**, 701-708.

Forslind, B. (1970). Biophysical studies of normal nail. *Acta Dermatol. Venereol.* **50**, 161-168.

Fraser, R. D., MacRae, T. P. and Rogers, G. E. (1972). *Keratins: Their Composition, Structure, and Biosynthesis*. Springfield, IL: Charles C. Thomas.

Fraser, R. D. B., MacRae, T. P. and Suzuki, E. (1976). Structure of keratin microfibril. *J. Mol. Biol.* **108**, 435-452.

Fudge, D. S., Szewciw, L. J. and Schwalb, A. N. (2009). Morphology and development of blue whale baleen: An annotated translation of Tycho Tullberg's classic 1883 paper. *Aq. Mamm.* **35**, 226-252.

Ginter-Summarell, C. C., Ingole, S., Fish, F. E. and Marshall, C. M. (2015). Comparative analysis of the flexural stiffness of pinniped vibrissae. *PLoS ONE* **10**, e0127941.

Goldbogen, J. A., Cade, D., Calambokidis, J., Friedlaender, A. S., Potvin, J., Segre, P. S. and Werth, A. J. (2017). How baleen whales feed: the biomechanics of engulfment and filtration. *Ann. Rev. Mar. Sci.* **9**, 367-386.

Gray, D. (1877). The feeding apparatus of the Greenland whale. *Land Water* **12**, 22.

Greenberg, D. A. and Fudge, D. S. (2012). Regulation of hard alpha-keratin mechanics via control of intermediate filament hydration: matrix squeeze revisited. *Proc. R. Soc. B Biol. Sci.* **280**, e2158.

Hearle, J. W. S. (2000). A critical review of the structural mechanics of wool and hair fibres. *Int. J. Biol. Macromol.* **27**, 123-138.

Hunt, K. E., Lysiak, N. S., Moore, M. J. and Rolland, R. M. (2016). Longitudinal progesterone profiles in baleen from female North Atlantic right whales (*Eubalaena glacialis*) match known calving history. *Cons. Physiol.* **4**, cow014.

Jensen, M. M., Saladrigas, A. H. and Goldbogen, J. A. (2017). Comparative three-dimensional morphology of baleen: cross-sectional profiles and volume measurements using CT images. *Anat. Rec.* **300**, 1942-1952.

Jorgensen, C. B. (1966). *Biology of Suspension Feeding*. Oxford: Pergamon Press.

Kasuya, T. and Rice, D. W. (1970). Notes on baleen plates and on arrangement of parasitic barnacles of gray whale. *Sci. Rep. Whales Res. Inst.* **22**, 39-43.

Kitchener, A. and Vincent, J. F. V. (1987). Composite theory and the effect of water on the stiffness of horn keratin. *J. Mat. Sci.* **22**, 1385-1389.

Lambertsen, R. H., Hintz, R. J., Lancaster, W. C., Hirons, A., Kreiton, K. J. and Moor, C. (1989). *Characterization of the functional morphology of the mouth of the bowhead whale, Balaena mysticetus, with special emphasis on the feeding and filtration mechanisms*. Report to the Department of Wildlife Management. Barrow, Alaska: North Slope Borough.

Lauder, G. V. (1985). Aquatic feeding in lower vertebrates. In *Functional Vertebrate Morphology* (ed. M. Hildebrand, D. M. Bramble, K. F. Liem and D. B. Wake), pp. 210-229. Cambridge: Harvard University Press.

Lee, M. (1998). *Baleen Basketry of the North Alaskan Eskimo*. Seattle: Univ. of Washington Press.

Lubetkin, S. C., Zeh, J. E., Rosa, C. and George, J. C. (2008). Age estimation for young bowhead whales (*Balaena mysticetus*) using annual baleen growth increments. *Can. J. Zool.* **86**, 525-538.

Lysiak, N. S. J., Trumble, S. J., Knowlton, A. R. and Moore, M. J. (2018). Fishing gear entanglement on a North Atlantic right whale (*Eubalaena glacialis*) using stable isotopes, steroid and thyroid hormones in baleen. *Front. Mar. Sci.* **5**, e168.

Marshall, R. C., Orwin, D. F. G. and Gillespie, J. M. (1991). Structure and biochemistry of mammalian hard keratin. *Electron Micros. Rev.* **4**, 47-83.

Mayo, C. A., Letcher, B. H. and Scott, S. (2001). Zooplankton filtering efficiency of the baleen of a North Atlantic right whale, *Eubalaena glacialis*. *J. Cet. Res. Mgmt.* **2**, 225-229.

McKittrick, J., Chen, P.-Y., Bodde, S. G., Yan, W., Novitskaya, E. E. and Meyers, M. A. (2012). The structure, functions, and mechanical properties of keratin. *J. Min. Met. Mat. Soc.* **64**, 449-468.

Moffat, R., Spriggs, J. and O'Connor, S. (2008). The use of baleen for arms, armour, and heraldic crests in medieval Britain. *Antiq. J.* **88**, 207-215.

Pace, R. M., Corkeron, P. J. and Kraus, S. D. (2017). State-space mark-recapture estimates reveal a recent decline in abundance of North Atlantic right whales. *Ecol. Evol.* **7**, 8730-8741.

Paig-Tran, E. W. M., Kleinteich, T. and Summers, A. P. (2013). Filter pads and filtration mechanisms of the devil rays: variation at macro and microscopic scales. *J. Morph.* **274**, 1026-1043.
Patek, S. N., Rosario, M. V. and Taylor, J. R. A. (2013). Comparative spring mechanics in mantis shrimp. *J. Exp. Biol.* **216**, 1317-1329.
Pautard, F. G. E. (1963). Mineralization of keratin and its comparison with the enamel matrix. *Nature* **199**, 531-535.
Pfeiffer, C. (1992). Cellular structure of terminal baleen in various mysticete species. *Aq. Mamm.* **18**, 67-73.
Pinto, S. J. D. and Shadwick, R. E. (2013). Material and structural properties of fin whale (*Balaenoptera physalus*) zwischensubstanz. *J. Morph.* **274**, 947-955.
Pivorunas, A. (1976). A mathematical consideration of the function of baleen plates and their fringes. *Sci. Rep. Whales Res. Inst.* **28**, 37-55.
Pomerleau, C., Matthews, C. J. D., Gobeil, C., Stern, G. A., Ferguson, S. H. and Macdonald, R. W. (2018). Mercury and stable isotope cycles in baleen plates are consistent with year-round feeding in two bowhead whale (Balaena mysticetus) populations. *Polar Biol.* **41**, 1-13.
Potvin, J. and Werth, A. J. (2017). Oral cavity hydrodynamics and drag production in balaenid whale suspension feeding. *PLoS ONE* **12**, e5220.
Prince, P. A. and Morgan, R. A. (1987). Diet and feeding ecology of Procellariiformes. In *Seabirds: Feeding Ecology and Role in Marine Ecosystems* (ed. J.P. Croxall), pp. 135-171. Cambridge: Cambridge University Press.
Rice, D. W. and Wolman, A. A. (1971). The life history and ecology of the gray whale (*Eschrichtius robustus*). *Am. Soc. Mamm.* **3**, 1-142.
Rubenstein, D. I. and Koehl, M. A. R. (1977). The mechanisms of filter feeding: some theoretical considerations. *Am. Nat.* **111**, 981-994.
Ruud, J. T. (1940). The surface structure of the baleen plates and a possible clue to age in whales. *Hval. Skrift.* **23**, 1-24.
Schell, D. M., Saupe, S. M. and Haubenstock, N. (1989). Bowhead whale (*Balaena mysticetus*) growth and feeding as estimated by $\delta^{13}C$ techniques. *Mar. Biol.* **103**, 433-443.
Simon, M., Johnson, M., Tyack, P. and Madsen, P. T. (2009). Behaviour and kinematics of ram filtration in bowhead whales (*Balaena mysticetus*). *Proc. Roy. Soc. B* **276**, 3819-3828.
St Aubin, D. J., Stinson, R. H. and Geraci, J. R. (1984). Aspects of the structure and composition of baleen, and some effects of exposure to petroleum hydrocarbons. *Can. J. Zool.* **62**, 193-198.
Stevenson, C. H. (1907). Whalebone: its production and utilization. *Bur. Fish. Doc.* **626**, 1-12.
Sumich, J. L. (2001). Growth of baleen in a rehabilitating gray whale calf. *Aq. Mamm.* **27**, 234-238.
Szewciw, L. J., de Kerkhove, D. G., Grime, G. W. and Fudge, D. S. (2010). Calcification provides mechanical reinforcement to whale baleen alpha keratin. *Proc. Roy. Soc. B* **277**, 2597-2605.
Taylor, A. M., Bonser, R. H. C. and Farrent, J. W. (2004). The influence of hydration on the tensile and compressive properties of avian keratinous tissues. *J. Mater. Sci.* **39**, 939-942.
van der Hoop, J. M., Corkeron, P., Kenney, J., Landry, S., Morin, D., Smith, J. and Moore, M. J. (2016). Drag from fishing gear entangling North Atlantic right whales. *Mar. Mamm. Sci.* **32**, 619-642.
Vogel, S. (1996). *Life in Moving Fluids*, 2nd edn. Princeton: Princeton Univ. Press.
Wang, B., Yan, W., McKittrick, J. and Meyers, M. A. (2016). Keratin: structure, mechanical properties, occurrence in biological organisms, and efforts at bioinspiration. *Prog. Mater. Sci.* **76**, 229-318.
Watkins, W. A. and Schevill, W. E. (1976). Right whale feeding and baleen rattle. *J. Mamm.* **57**, 58-66.
Werth, A. J. (2000). Marine mammals. In *Feeding: Form, Function, and Evolution in Tetrapod Vertebrates* (ed. K. Schwenk), pp. 475-514. New York: Academic Press.
Werth, A. J. (2001). How do mysticetes remove prey trapped in baleen? *Bull. Mus. Comp. Zool.* **156**, 189-203.
Werth, A. J. (2004). Models of hydrodynamic flow in the bowhead whale filter feeding apparatus. *J. Exp. Biol.* **207**, 3569-3580.
Werth, A. J. (2012). Hydrodynamic and sensory factors governing response of copepods to simulated predation by baleen whales. *Int. J. Ecol.* **2012**, 208913.
Werth, A. J. (2013). Flow-dependent porosity and other biomechanical properties of mysticete baleen. *J. Exp. Biol.* **216**, 1152-1159.
Werth, A. J. and Potvin, J. (2016). Baleen hydrodynamics and morphology of cross-flow filtration in balaenid whale suspension feeding. *PLoS ONE* **11**, e0150106.
Werth, A. J. and Ito, H. (2017). Sling, scoop, squirter: anatomical features facilitating prey transport, concentration, and swallowing in rorqual whales (Mammalia: Mysticeti). *Anat. Rec.* **300**, 2070-2086.
Werth, A. J., Harriss, R. W., Rosario, M. V., George, J. C. and Sformo, T. L. (2016a). Hydration affects the physical and mechanical properties of baleen tissue. *Roy. Soc. Open Sci.* **3**, 160591.
Werth, A. J., Straley, J. M. and Shadwick, R. E. (2016b). Baleen wear reveals intraoral water flow patterns of mysticete filter feeding. *J. Morph.* **277**, 453-471.
Werth, A. J., Potvin, J., Shadwick, R. E., Jensen, M. M., Cade, D. E. and Goldbogen, J. A. (2018). Filtration area scaling and evolution in mysticetes: trophic niche partitioning and the curious cases of sei and pygmy right whales. *Biol. J. Linn. Soc.*
Werth, A. J., Rita, D., Rosario, M. V., Moore, M. J. and Sformo, T. L. (2018). Data from: How do baleen whales stow their filter? A comparative biomechanical analysis of baleen bending. *Dryad Digital Repository*. https://doi.org/10.5061/dryad.73rm81p.
Williamson, G. R. (1973). Counting and measuring baleen and ventral grooves of whales. *Sci. Rep. Whales Res. Inst.* **24**, 279-292.
Young, S. (2012). The comparative anatomy of baleen: evolutionary and ecological implications. *MSc thesis*, San Diego State University.
Zweers, G., de Jong, F., Berkhoudt, H. and Vanden Berge, J. C. (1995). Filter feeding in flamingos (*Phoenicopterus ruber*). *Condor* **97**, 297-324.